High-performance ZnO humidity sensor synthesized by coprecipitation with PVP as surfactant for human respiration detection*

MAN Jianping[1,2], GU Weiyuan[1,2], HU Ziyan[1], DOU Xiaozong[1], and ZHANG Hongyan[1,2]**

1. *Xinjiang Key Laboratory of Solid State Physics and Devices, Xinjiang University, Urumqi 830046, China*
2. *School of Physics Science and Technology, Xinjiang University, Urumqi 830046, China*

(Received 17 June 2022; Revised 2 September 2022)
©Tianjin University of Technology 2023

A high-performance zinc oxide (ZnO)/polyvinylpyrrolidone (PVP) humidity sensor was prepared by simple coprecipitation method with PVP as surfactant. The coprecipitation method has low reaction temperature, little energy consumption and simple preparation, which is suitable for large-scale production. The PVP makes sample's surface with more hydroxyl and oxygen vacancies than pure ZnO, which can absorb more water molecules and promote the decomposition of water molecules into H_3O^+ to form effective ion conduction. When the molar ratio of PVP to ZnO is 1:1, the ZnO/PVP humidity sensor has low hysteresis (~4.2%), short response/recovery time (9/10 s), excellent stability and high sensitivity with more than 4 orders of magnitude in relative humidity (RH) range from 11% to 95%. Moreover, the ZnO/PVP humidity sensor can distinguish different respiratory states of human body, which has a potential in monitoring and prevention of respiratory diseases.

Document code: A **Article ID:** 1673-1905(2023)01-0001-7

DOI https://doi.org/10.1007/s11801-023-2105-2

Humidity sensors have been applied to food monitoring, manufacturing production, weather forecast, drug storage, respiratory detection and so on[1]. With the increase of application areas, the demand for humidity sensors with high stability, good sensitivity and easy mass production is increasing. In recent years, many sensitive materials have been used into humidity sensors such as ceramics, carbon nanocoils (CNCs), metal oxides, graphene oxide (GO) and electrolytes[2]. Among them, metal oxides semiconductors have received extensive attention from researchers because of their easy preparation, low-cost and high stability[3]. Zinc oxide (ZnO) with 60 meV exciton binding energy and 3.2—3.3 eV band gap[4] is a typical metal oxide in semiconductor, which has been widely used in sensitive materials due to abundant surface oxygen vacancies than other metal oxides[5,6].

There are various methods to synthesize ZnO materials, such as hydrothermal[7], sol-gel[8], electro-chemical, coprecipitation and microemulsion method. Compared with the above methods, coprecipitation method requires low reaction temperature and simple synthesis, which makes it easy to control size and crystallinity of ZnO during fabrication, and makes it suitable for industrial large-scale production[9].

It has been reported that oxygen vacancies and hydroxyl groups on the surface of material can effectively enhance ability to adsorb water molecules to promote the sensitivity of sensor. Nevertheless, pure ZnO doesn't have enough hydroxyl group, which limits its application in humidity detection. Strong water solubility and hygroscopicity of surfactants can enhance the amount of hydroxyl groups on external contact surface of material. Therefore, an effective way to improve the shortcomings of ZnO is to add surfactants into the reaction process[10]. The polyvinylpyrrolidone (PVP) has strong binding ability to water molecules due to its microstructure and water solubility. Moreover, PVP has a fibrous structure which makes it easier to transfer water molecules, hence to improve water absorption capacity of ZnO[11]. In addition, it has high dielectric constant, moderate conductivity, as well as to be non-toxic, low price and easy to process, which makes it an ideal surfactant for the preparation of ZnO.

In this paper, a simple coprecipitation synthetic route was used to prepare high performance ZnO humidity sensor using PVP as surfactant (ZnO/PVP). The addition of PVP increases the number of hydroxyl groups and oxygen vacancies on ZnO surface, which enhances adsorption capacity and dissociation capacity of ZnO to

* This work has been supported by the National Natural Science Foundation of China (No.62064011).
** E-mail: zhanghyxj@163.com

water molecules. Compared with the ZnO humidity sensors reported in literature, the ZnO/PVP humidity sensor prepared by coprecipitation method is more beneficial to large-scale industrial production. Furthermore, ZnO/PVP humidity sensor can effectively distinguish different breathing states of human normal breathing by the change of its impedance and frequency.

Zinc acetate ($Zn(CH_3COO)_2·2H_2O$), PVP (molecular weight of 20 000) and sodium hydroxide (NaOH) were obtained from Sangon Biotech (China). All chemical reagents used were of analytical grade (AR) without any further purification. Deionized water was used throughout all the experiments.

A simple coprecipitation method was used to synthesize ZnO. 50 mg of $Zn(CH_3COO)_2·2H_2O$ and a certain amount of PVP (0 mg, 12.6 mg, 25.2 mg and 30.24 mg) were dissolved in 70 mL deionized water with molar ratios of 1: 0, 1: 0.5, 1: 1 and 1: 1.2, respectively, and stirred magnetically about 10 min. Then 80 mg NaOH solution was slowly added into mixed reactants and stirred for 20 min. After 12 h, the resulting products were centrifuged and washed with deionized water and ethanol repeatedly until the supernatant was transparent. The precipitation was dried at 95 °C to produce white ZnO/PVP powder with different contents of PVP as surfactant, which are denoted as ZnO, ZP0.5, ZP1 and ZP1.2, respectively.

Crystal structure of the sample was characterized by X-ray diffraction (XRD, Bruker D8 Advance, Germany) with Cu-Kα radiation operating at 40 kV in a scanning range from 20° to 80°. Surface microstructure of the sample was analyzed by scanning electron microscope (SEM, S-4800, Japan). Molecular vibration on surface of the sample was investigated by Fourier transform infrared spectroscopy (FTIR, Bruker-V Vertex 70, Germany). Elemental composition of the prepared sample was analyzed by X-ray photoelectron spectrometer (XPS, Thermo ESCALAB 250Xi, USA), and monochromatic Al-Kα 1 486.6 eV radiation was used as an excitation source.

Firstly, the prepared ZnO sample was placed in an agate mortar, followed by the adding of deionized water water in a 5: 1 ratio and grinding to a paste. Secondly, the paste was spreaded on Ag-Pd cross electrode with a small brush and desiccated at 60 °C for 50 min in electric thermostatic drying oven to prevent the sample from falling off. Finally, the humidity performance of samples was measured at room temperature (25 °C) by a Zennium workstation (CIMPS-2, Zahner) with a voltage set to be alternating current (AC) 1 V and measurement frequency between 40 Hz and 100 kHz. Moreover, the different humidity environments were controlled by different supersaturated aqueous solutions of LiCl, $MgCl_2$, K_2CO_3, NaBr, NaCl, KCl and KNO_3 to yield 11%, 33%, 43%, 59%, 75%, 85% and 95% relative humidity (RH), respectively.

In Fig.1(a), characteristic peaks at 2θ values of all samples are 31.7°, 34.4°, 36.3°, 47.5°, 56.6°, 62.3°, 66.5°, 67.9°, 69.1° and 77.2°, respectively, which correspond to lattice planes (100), (002), (101), (102), (110), (103), (200), (112), (201) and (202) for hexagonal phase of ZnO (JCPDS No.36-1451). Diffraction peak intensities of all ZnO samples decrease with the increase of PVP concentration. Higher PVP concentration can produce stronger steric hindrance effect and further increase the viscosity of the material, which can cause slower nucleation rate and crystal growth rate[12], resulting in poor crystallinity of ZP1 and the worst crystallinity of ZP1.2. For Fig.1(b), the peak at 423 cm^{-1} is attributed to Zn-O stretching vibration in ZnO crystal. The characteristic peaks at 923 cm^{-1} and 1 424 cm^{-1} are consistent with the deformation of C-O and the bending vibration of O-H bond, respectively, while the peaks at 1 011 cm^{-1} and 1 044 cm^{-1} suggest the C-O stretching vibration. The above four peaks are due to the addition of $Zn(CH_3COO)_2·2H_2O$. Characteristic absorption peaks are located at 3 407 cm^{-1}, 2 978 cm^{-1}, 1 670 cm^{-1} and 1 287 cm^{-1}, respectively, which are attributed to O-H stretching, CH_2 asymmetric stretching, C=O tensile, O-H bending and C-N tensile vibration belt. Tensile vibration and bending vibration of O-H are due to hydroxyl vibration caused by strong adsorption of PVP or ZnO on water molecules, while tensile vibration of C-O bond or C-N bond is due to the addition of PVP in the experiments. The peak pattern at 3 407 cm^{-1} becomes broader and stronger with the increase of PVP content, indicating that PVP increases -OH content on surface of the sample, which can enhance adsorption capacity of ZnO to water molecules[13].

In Fig.1(c) and Fig.1(d), O 1s can be decomposed into three significant oxygen species O_1, O_2 and O_3, which represent lattice oxygen, oxygen vacancy and free oxygen (O_3), respectively. Compared with ZnO and ZP1, the proportions of O_1, O_2 and O_3 change from 48.1%, 24.2% and 27.7% to 43.3%, 34.4% and 22.3%, respectively. The percentage content of O_1 in ZnO is higher than ZP1, which can be attributed to the better crystallinity of ZnO, and the results are consistent with XRD. O_2 helps the material capture more water molecules and easily decompose the surface water molecules into hydroxyl, which enhances proton transport on surface of the material and improves sensitivity of the sensor[14]. The proportion of O_2 in ZP1 is higher than ZnO, meaning that ZP1 has stronger ability to adsorb water molecules to enhance surface charge density.

Fig.2(a) and (b) demonstrate that pure ZnO is composed of micron-sized particles ranging from 0.1 μm to 0.5 μm and has a small amount of aggregation. Fig.2(c) and (d) show that ZP1 is composed of many agglomerated micron-sized particles ranging from 0.08 μm to 0.6 μm. Compared with ZnO, ZP1 particle size is larger, agglomeration phenomenon is serious, which may be due to PVP increases surface viscosity of ZP1. Moreover, more voids and pores are generated in ZP1, which is conductive to the adsorption of more water molecules.

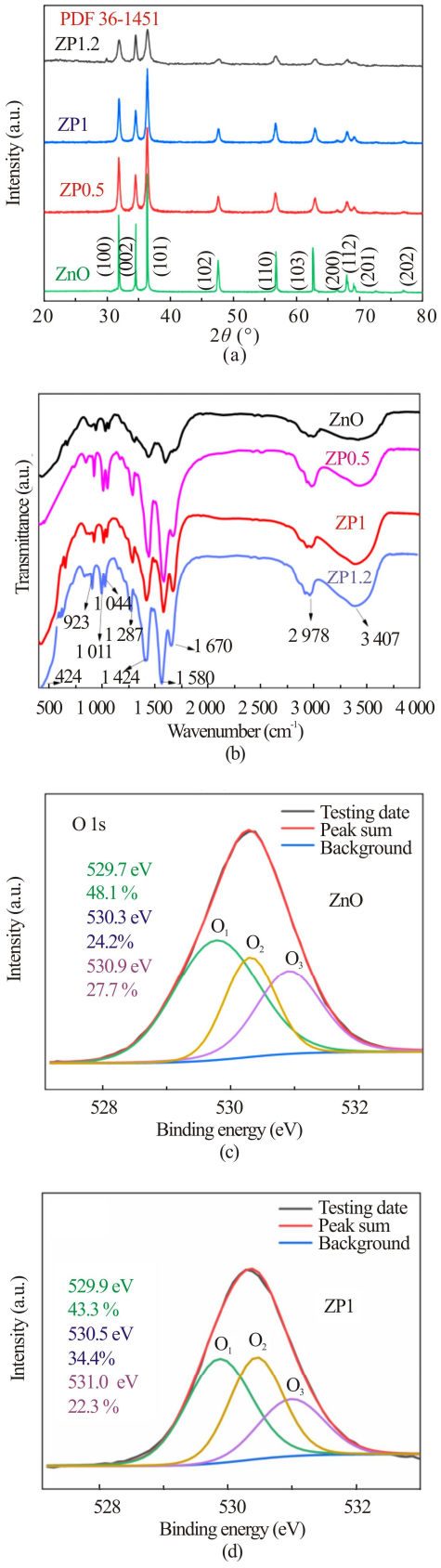

Fig.1 (a) XRD spectra of ZnO, ZP0.5, ZP1 and ZP1.2; (b) FTIR spectra of ZnO, ZP0.5, ZP1 and ZP1.2; XPS spectra for O 1s of (c) ZnO and (d) ZP1

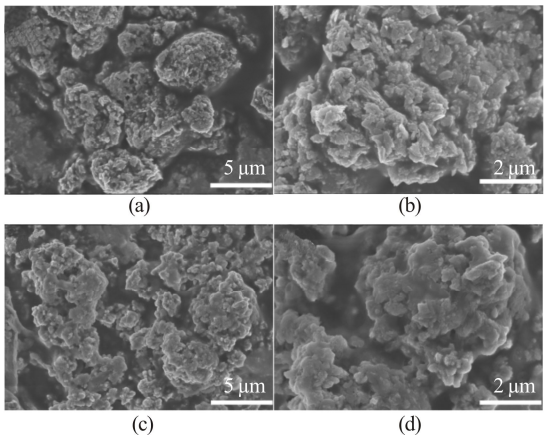

Fig.2 (a) SEM images of ZnO and (b) corresponding details; (c) SEM images of ZP1 and (d) corresponding details

Fig.3(a) shows that impedance of ZnO/PVP is apparently lower compared to pure ZnO in the range from 11% to 95% RH, which is attributed to the increase of hydroxyl groups on ZnO surface after PVP addition. More hydroxul groups adsorbed more water molecules to increase surface charge density and reduce impedance of the material. In addition, sensitivity of the sample is enhanced with the increasing amount of PVP, which results in more oxygen vacancies on ZnO/PVP surface to improve water absorption capacity and enhance the ability to decompose water molecules into H_3O^+. However, the sensitivity of ZP1.2 is high but the linearity is poor. Over-high PVP concentration will increase viscosity of ZP1.2 and hinder proton migration, which means that ZP1.2 has stronger inhibition to ion transfer, leading to the deterioration of linearity. Results show that compared with ZnO, the sensitivity of ZP1 is increased by 3 orders of magnitude. In addition, the linearity of ZP1 is also the best in all samples.

Fig.3(b) describes the changes of impedance for ZP1 with various test frequencies between 40 Hz and 100 kHz. The impedance of the sample shows weak change when test frequency is 100 kHz, 10 kHz and 1 kHz, which is due to the current changes direction before the water molecules are polarized. The sensitivity of ZP1 reaches nearly 5 orders of magnitude when test frequency is 40 Hz, but its linearity is poor and impedance is unstable. Only when the test frequency is 100 Hz, the change in the impedance of ZP1 reaches over 4 orders of magnitude with excellent stability, so 100 Hz is the optimal test frequency of ZP1 sensor.

Fig.3(c) and (d) respectively describe hysteresis curves of ZnO and ZP1 when RH ranges from 11% to 95%. In order to detect current humidity, previously absorbed humidity of sensor needs to be eliminated when environmental humidity decreases, and this process is called desorption. For ZnO or ZP1, the impedance of the

sensors during desorption is significantly smaller than adsorption. This can be attributed to the desorption of ZnO for water molecules is an endothermic reaction, adsorption and desorption require different energy, so it takes more external energy to pull the water molecules off the sensor surface[15]. The value difference of characteristic curves of adsorption and desorption is called hysteresis, and the hysteresis value can be calculated by the following formula, $\{[\log(R_{Ad})-\log(R_{De})]/\log(R_{Ad})\}\times 100\%$, where R_{Ad} and R_{De} represent the impedance value differences between adsorption curve and desorption curve in same humidity environment[16]. For Fig.3(c) and (d), the largest hysteresis errors of ZnO and ZP1 are 8.1% (75% RH) and 4.2% (75% RH), respectively. The smaller the hysteresis, the better the sensor performs, which means ZP1 sensor has excellent reversible sensing characteristics.

Response and recovery time of the sensor are determined by the sensor reaches 90% of impedance change in the process of adsorption and desorption process. Fig.3(e) and (f) describe the response and recovery time of ZnO and ZP1, which read to be 30/18 s and 9/10 s, respectively. More hydroxyl and oxygen vacancies on the surface of ZP1 make it not only adsorb more water molecules, but also accelerate the decomposition of water molecules, effectively reducing its response and recovery time.

Fig.4(a) indicates the impedance changes of ZP1 over six cycles of 10 days each. There are only slight changes of impedance observed in each different humidity environment, indicating that ZP1 sensor has good stability in different humidity environments.

During sensor detection, sensor's response is defined as follows, $Response=R_A/R_T$, where R_A and R_T represent impedances in air and target, respectively. Fig.4(b) indicates that responses of ZP1 to different gases at 500 pm to be 6.2—10.4. The response of ZP1 is only 0.3 and 0.2 in the environment of pure N_2 and CO_2. Responses of ZP1 reach 352 and 1 287 in 60% RH and 90% RH, respectively, which mean that ZP1 sensor almost eliminates interference of different gases and expel the interference of exhaled gas. Humidity of the air inhaled by human body at room temperature ranges from 30% to 60%, and the humidity of the air exhaled by human body generally exceeds 90%. It almost eliminates the interference of different gases to ZP1 and achieves accurate measurement when ZP1 humidity sensor is used for human breath detection, which provides broad application in the field of breath detection.

Fig.4(c) shows the frequency of three adults fast breathing is about 0.40 Hz and its peak strength is relatively weak, which is due to the small number of water molecules are absorbed by the sensor, leading to small changes in impedance. Fig.4(d) depicts that the frequency of three adults normal breathing is about 0.26 Hz, and its peak intensity is increased compared with fast breathing, which can be attributed to more water molecules are absorbed by the sensor. Fig.4(e) indicates that the frequency of three adults under slow breathing is

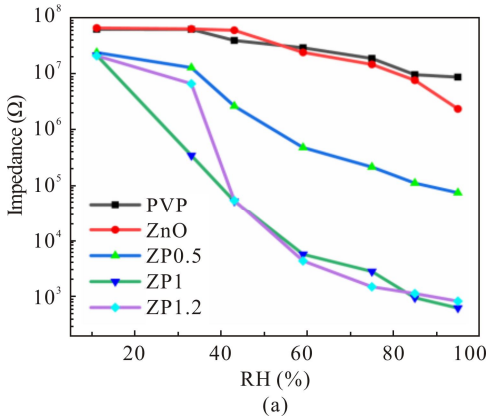

(a)

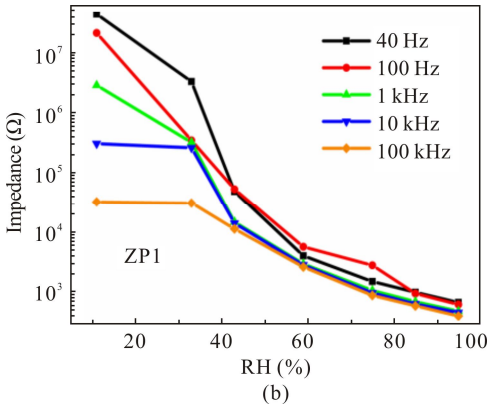

(b)

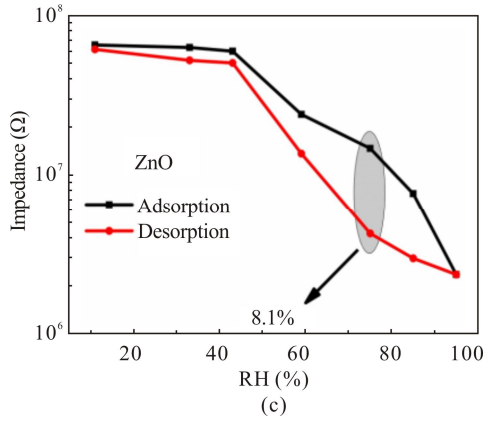

(c)

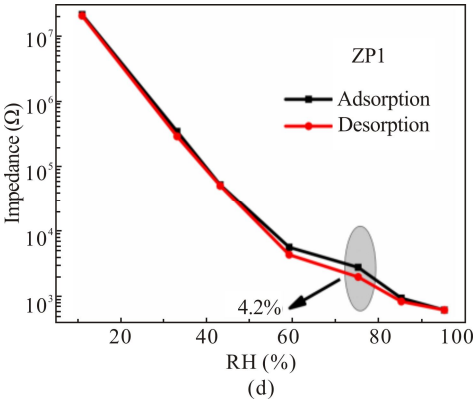

(d)

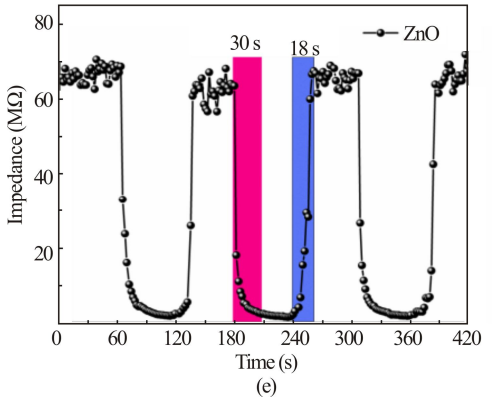

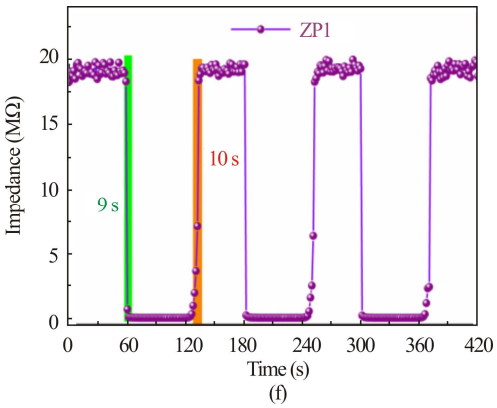

Fig.3 (a) Humidity sensitive properties of different molar ratios of ZnO and PVP; (b) Changes of impedance based on ZP1 at different frequencies; Hysteresis of (c) ZnO and (d) ZP1 in the RH range from 11% to 95%; Response and recovery time of (e) ZnO and (f) ZP1 in the RH range from 11% to 95%

about 0.16 Hz. Among three adults, the sensor absorbs more water molecules than fast or normal breathing process, resulting in larger impedance changes. Therefore, ZP1 sensor can detect the above three different nose breathing states through the change of frequency and impedance. In Fig.4(f), the accuracy of the sensor can be expressed as $Q=(\Delta Z_1/Z)\times 100\%$, where Z represents the impedance when 2 mm from the nose (full scale impedance), ΔZ_1 represents the absolute value of the difference between the measured impedance range and full scale resistance. According to the calculation, the accuracy of the sensor is about 85% and 29% when the breathing distance is 10 mm and 20 mm from the nose, so it can be seen that the measurement distance is 2—10 mm.

Measured by AC impedance method in range from 11% to 95% RH, complex impedance spectrum and its equivalent circuit diagram of ZP1 are shown in Fig.5. The interaction process of ZP1 with humidity can be divided into three parts. Fig.5(a) shows the curve of impedance tends to a straight line at 11% RH, and the equivalent circuit is a constant phase element (CPE). At this process, water molecules are chemically adsorbed on ZP1 surface, but no sequential adsorption has been formed in chemisorbed water layer. As RH increases from 33% to 59%, the equivalent circuit is connected in

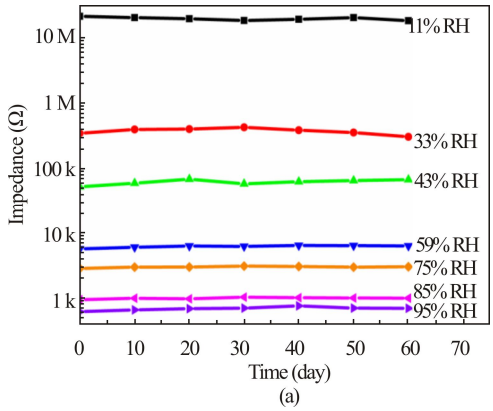

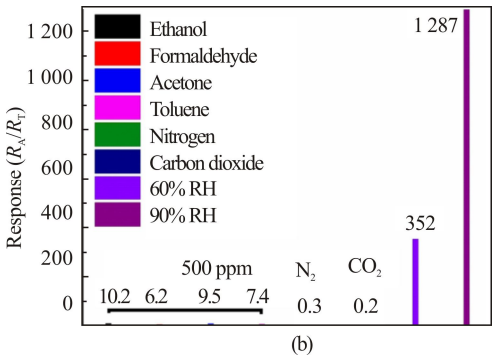

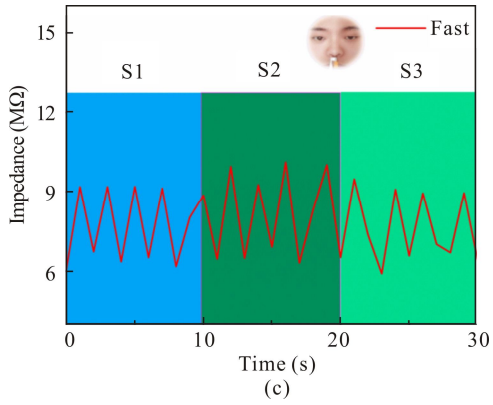

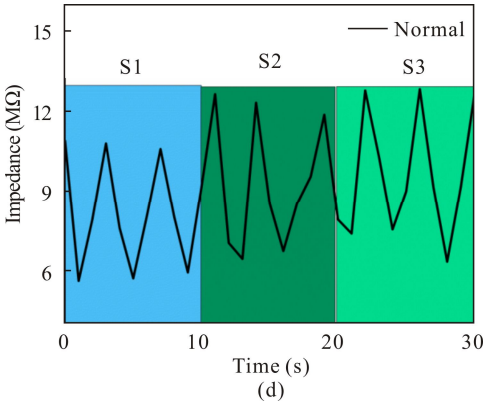

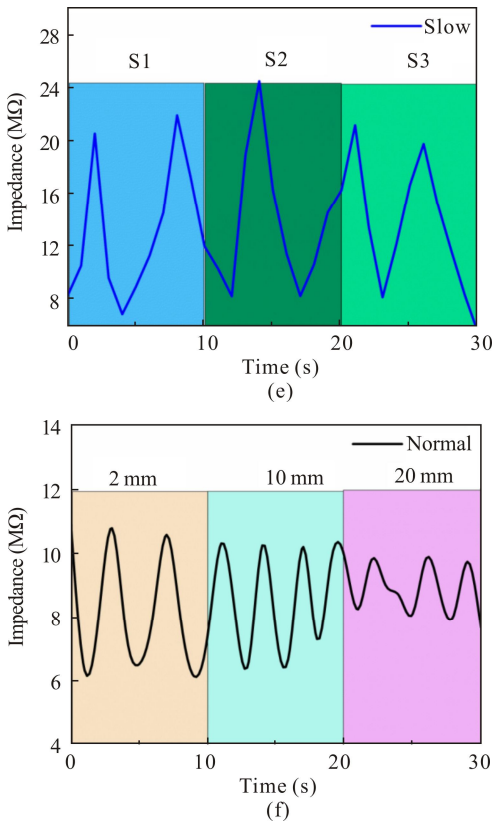

Fig.4 (a) Impedance stability test of ZP1 humidity sensor in RH range from 11% to 95%; (b) Response of ZP1 humidity sensor to different gases and RH values; Impedance changes of ZP1 humidity sensor at 2 mm from nose when detecting three adults with (c) fast breathing, (d) normal breathing, and (e) slow breathing; (f) Accuracy of ZP1 humidity sensor at different distances from nose

series with Warburg impedance (Z_W) after the resistor and capacitor are in parallel. The left half of the curve is an arc, which represents charge transfer caused by hopping transport of protons. Water molecules are continuously chemically adsorbed on ZP1 sensor surface to form continuous water molecular layers, resulting in the increase of capacitance and the decrease of impedance in the equivalent circuit. A straight diagonal line occurs at the end of the arc, which is denoted as Z_W, and it is attributed to the improvement of diffusion of electrically active substance at the electrode/sensor film interface. In this case, sensing characteristics of ZP1 humidity sensor are controlled by Z_W. As RH further increases, the curve almost becomes a straight line as shown in Fig.5(c). Currently, the equivalent circuit is capacitor C in series with Z_W. Water molecules absorbed on the sample further increase and the chemical adsorption layer is covered by physical adsorption layer. Electrons will be released to promote electrolytic generation of H^+ and OH^- by water molecules. The surrounding water molecules are bonded to one another by hydrogen bonds and induced to rotate by H^+ near the water molecules, and alternate changes of covalent bonds and hydrogen bonds lead to proton transfer. In this case, the sensing characteristics of the sensor are completely determined by Z_W and the material transfer in the form of electrolysis becomes dominant.

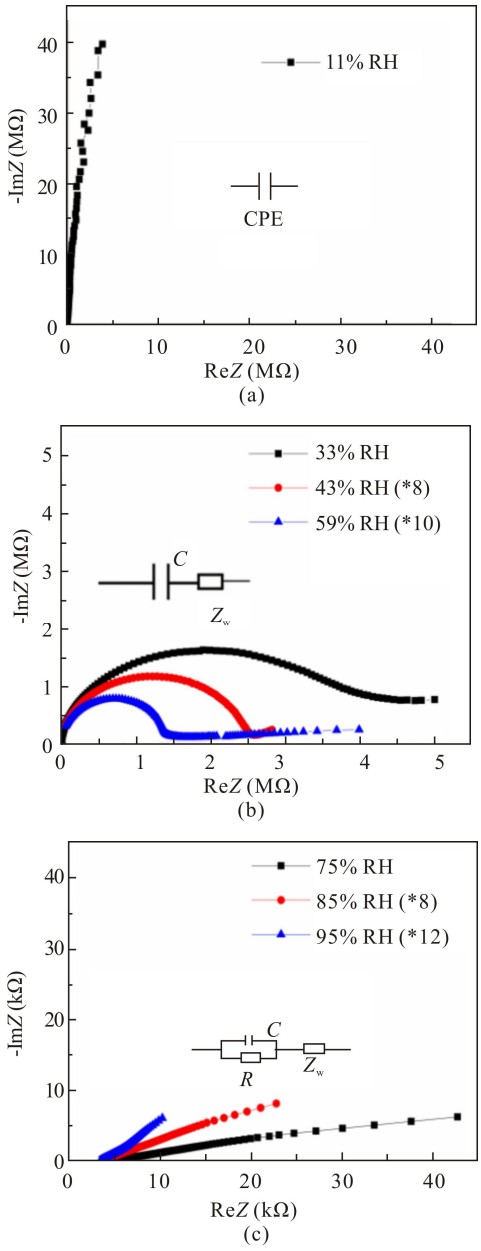

Fig.5 Complex impedance spectra based on ZP1 humidity sensor and corresponding equivalent circuits measured at RH of (a) 11%, (b) 33%, 43%, 59%, and (c) 75%, 85%, 95%, respectively

A high performance ZnO humidity sensor was fabricated by a simple coprecipitation method using PVP as surfactant. Experimental results show that PVP significantly increases the number of oxygen vacancies and hydroxyl groups on ZnO surface. Through synergistic action of vacant oxygen with hydroxyl group, a great deal of water molecules are adsorbed on surface of ZnO to form effective ion conduction, which improves sensitivity,

linearity and response/recovery speed of ZP1 humidity sensor. Furthermore, ZnO/PVP humidity sensor can effectively distinguish different breathing states of human when it is used for respiratory detection. In short, this coprecipitation method for the preparation of high-performance ZnO humidity sensor is conducive to large-scale industrial production.

Statements and Declarations

The authors declare that there are no conflicts of interest related to this article.

References

[1] KULWICKI B M. Humidity sensors[J]. Journal of the American Ceramic Society, 1991, 74：697-708.

[2] TAI H L, WANG S, DUAN Z H, et al. Evolution of breath analysis based on humidity and gas sensors：potential and challenges[J]. Sensors and actuators B：chemical, 2020, 318：128104.

[3] KILIC B, CELIK V. Self-assembled growth of tandem nanostructures based on TiO_2 mesoporous/ZnO nanowire arrays and their optoelectronic and photoluminescence properties[J]. Applied physics A, 2015, 119：783-790.

[4] SHINDE S S, SHINDE P S, OH Y W, et al. Structural, optoelectronic, luminescence and thermal properties of Ga-doped zinc oxide thin films[J]. Applied surface science, 2012, 258：9969-9976.

[5] HSU S N F, CHANG M, HSU K T. Rapid synthesis of ZnO dandelion-like nanostructures and their applications in humidity sensing and photocatalysis[J]. Materials science in semiconductor processing, 2014, 21：200-205.

[6] LI Y J, ZHANG H M. Research on the preparation and growth mechanism of ZnO micro/nano nails[J]. Optoelectronics letters, 2018, 14：248-251.

[7] PANDA S, BISWAS C, PAUL K S. A comprehensive review on the preparation and application of calcium hydroxyapatite：a special focus on atomic doping methods for bone tissue engineering[J]. Ceramics international, 2021, 47：28122-28144.

[8] BEZZI G, CELOTTI G, LANDI E, et al. A novel sol-gel technique for hydroxyapatite preparation[J]. Materials chemistry and physics, 2003, 78(3)：816-824.

[9] RAGHUVEER V, MANTHIRAM A. Role of TiB_2 and Bi_2O_3 additives on the recharge ability of MnO_2 in alkaline cells[J]. Journal of power sources, 2006, 163：598-603.

[10] LI P, ZHANG H Y, LI Z J, et al. Effect of surfactants on morphology, structure and photoluminescence properties of Eu-doped ZnO microsphere[J]. Optoelectronics letters, 2020, 16：293-297.

[11] KHAN H U, TARIQ M, SHAH M, et al. Designing and development of polyvinylpyrrolidone-tungsten trioxide (PVP-WO_3) nanocomposite conducting film for highly sensitive, stable, and room temperature humidity sensing[J]. Materials science in semiconductor processing, 2021, 134：106053.

[12] YU Z J, KUMAR M R, SUN D L, et al. Large scale production of hexagonal ZnO nanoparticles using PVP as a surfactant[J]. Materials letters, 2016, 166：284-287.

[13] MA X S, WANG D H, CUI Y Z, et al. A novel hydrophilic conjugated polymer containing hydroxyl groups：syntheses and sensing performance for NACs in aqueous solution[J]. Sensors and actuators B：chemical, 2017, 251：851-857.

[14] YU S G, ZHANG H Y, CHEN C, et al. Investigation of humidity sensor based on Au modified ZnO nanosheets via hydrothermal method and first principle[J]. Sensors and actuators B：chemical, 2019, 287：526-534.

[15] ZHOU J, XIAO X, CHENG X F, et al. Surface modification of polysquaraines to sense humidity within a second for breath monitoring[J]. Sensors and actuators B：chemical, 2018, 271：137-146.

[16] XIE X J, SI R J, ZHENG J, et al. Synthesis of ZnO/NiO hollow spheres and their humidity sensing performance[J]. Journal of alloys and compounds, 2021, 879：160487.